Analysis of floating-head heat exchanger bolts failure

B. Gligorijević[1,*], B. Katavić[1], A. Alil[1], B. Jegdić[1], M. Ristić[1], and M. Prokolab[1]
[1]Institut Goša, Milana Rakića 35, 11000 Belgrade Serbia
*bojan.gligorijevic@institutgosa.rs

Abstract.

As-received floating-head heat exchanger bolts were broken (BB) and deposite-coated. The aim was to estimate a cause of their failure. The new bolts of the same material were used as a reference material (reference bolt – RB). After visual and radiographic examination, their chemical composition, structure and room-temperature mechanical properties were determined and compared. Comparison was made with the values set by standard, as well. Afterwards, fractography was performed on fractured surfaces of tensile specimens and originally (during exploitation) BBs to try to get an impression about bolts failure mechanism. Qualitative analysis of deposite was employed in order to confirm was there any possible influence of surroundings during their failure in terms of corrosion-assisted cracking. Chemical composition of RB and BB materials was analyzed by use of spectrophotometry and structure properties with light optical microscope (LOM). Fractured surfaces of tensile specimens and of BBs, as well as deposite chemistry, were analyzed by use of Scanning Electron Microscopy with Energy Dispersive System (SEM-EDS). BBs had an approximately three times higher sulphur content and lesser manganese content, lower ductility and higher strength values comparing to those of the RBs. Generally, fracture surfaces of both, RB and BB tensile specimens have a similar rosette-like macro-appearance. The only difference is that the radial marks in the case of the RBs are rougher. The surface has a more fibrous area and shear lip presence. Fracture mode can be characterized as dimple rupture and micromechanism as microvoid coalescence. In the case of BB tensile specimens, the mixed presence of dimples and cleavage facets was noticed. The macrofractography of originally broken surfaces shows a rough and complex topography of fracture surfaces indicating on a possibility that bolts failure has been a result of complex loading conditions. Presence of sulphur- and chlorine-containing particles on the fracture surfaces of BBs and in deposite reveals a possibility that failure was environmentally-assisted.

Keywords: bolts, chemical and structure analysis, mechanical testing, SEM-EDS, fracture mechanism

1. Introduction

One of the most common failures in the industry would happen due to the brittle fracture known as sulphide stress cracking (SSC) when the surrounding environment contains sulphur compounds such as H_2S [1].The salts and sulfide compounds dissolved in crude oil can provoke the formation of a corrosive aqueous solution whose chemical composition involves the presence of both hydrochloric acid (HCl) and hydrogen sulfide (H_2S). This corrosion aqueous solution is very aggressive causing varied damages on carbon steel during plant operation in primary distillation plants. Several previous studies have been performed related to the corrosion process of iron and steel in H_2S solutions. In H_2S-containing solutions, the corrosion process of metal may be accompanied by the formation of sulfide film on the metal surface and leads to more complicated corrosion behavior. [1, 2, 3, 4, 5]

Damage of metal parts and constructions is a complex process which takes place with effect of one or more mechanisms, such as: surface damages (corrosion, wear); distortion (elastic and plastic) and fracture. These damages do not take effect individually, but in mutual interaction. Fracture, which is a most severe form of material damage, is under influence of numerous factors, such as: mechanical stresses, temperature, composition and properties of atmosphere, shapes and dimensions of a part or construction; structure and properties of material and quality of surface. In order to determine the cause of fracture, in this paper, the specimens of new bolts (reference bolts = RB) and bolts that were broken

during the exploitation (broken bolts = BB) were tested. It is important to note that information other than temperature and pressure of gas in the heat exchanger, where bolts were located, is not known. The aim of this study is to analyze floating-head exchanger bolts failure on the basis of preliminary obtained results.

2. Materials and Methods

As-received bolts, used in this study, are made of ASTM A 193 B7 steel with approximately 19 mm in diameter and 225 mm or 170 mm in length. Their average chemical composition was determined by use of spectrophotometry (Table 1). The as-received bolts were probably in rolled and quenched and tempered condition according to structure (Figure X) and mechanical properties (Table 2).

In order to estimate the cause of their failure they were firstly subjected to detailed visual examination and radiographic measurements by γ-rays, according to ISO 5579 standard. From these measurements and appearance of complex fractured surfaces, as well as presence of bolt deposite, it was decided to estimate the quality of BBs and to perform chemical analysis of bolt's deposite and fractured surfaces of broken bolts. Here, by quality it is considered the information about presence of impurities, microcavities, microcracks, primary and secondary structure and mechanical properties. These can give the overall picture about fracture resistance of broken bolt material when compared to reference bolt material and standard values. Additionally, the fracture resistance is estimated from results of fractography of fractured surfaces of tensile and originally broken specimens. The chemical analysis of bolt deposite and fractured surfaces has given the information about presence of corrosion environment.

The samples for structure analysis were taken from different parts of RBs and BBs by cutting in radial direction. Subsequently, they were grinded by SiC abrasive paper and polished down to 1 μm using Al_2O_3 suspension. Primary structure was revealed by use of Oberhoffer's reagent, while secondary structure with 2% Nital. The presence of microcavities and microcracks was analyzed on polished surfaces by use of Scanning Electron Microscopy with Energy Dispersive System (SEM-EDS), as well as fractography, fractured surfaces chemistry and deposite chemistry. SEM-EDS analysis was performed at the University of Belgrade – Faculty of Mining and Geology, using a JEOL JSM–6610LV scanning electron microscope connected with the INCA350 energy-dispersion X-ray analysis unit. The acceleration voltage of 20 kV was used. Before SEM-EDS analysis was performed all surfaces to be analyzed were 20 nm gold coated in a high vacuum chamber by use of sputter coater device.

Tensile testing of bolts was carried out according to SRPS EN 10002-1 using short proportional test specimens with 7 mm in diameter, which were taken in axial direction. The Vickers hardness measurements (HV5) were performed on polished samples in radial direction, according to SRPS C.A4.030.

3. Results and Discussion

3.1. Visual examination and radiography measurements

Preliminary visual examination of RBs hasn't shown any irregularities presence (Figure 1a). BBs were deposite-coated (Figure 1b and Figure 1c). Color of deposite was predominantly black (probably result of organic species presence). the light-gray and

brown-red deposite color was observed mixing with black deposite (probably the result of corrosion processes). Generally, all bolts had a complex topography of fractured surfaces (Figure 3). Common for all bolts was that fracture was initiated in the root thread. After initiation, cracks propagated through the stud in radial direction, sometimes abrubtly changing the planes of propagation to the final fracture (Figure 2).

Radiography measurements have shown that several broken bolts had volume cracks 4 mm to 15 mm long, which expand in radial direction, and few in axial direction.

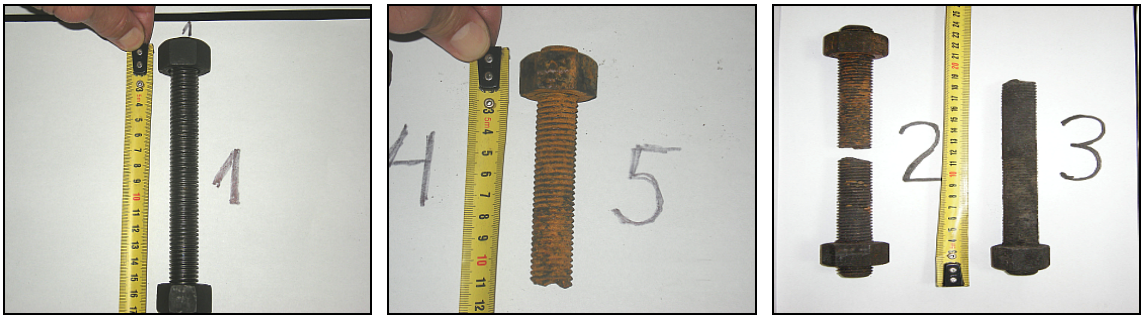

(a) (b) (c)

Figure 1. As-received (a) reference bolt (RB) and (b) and (c) broken bolts (BBs).

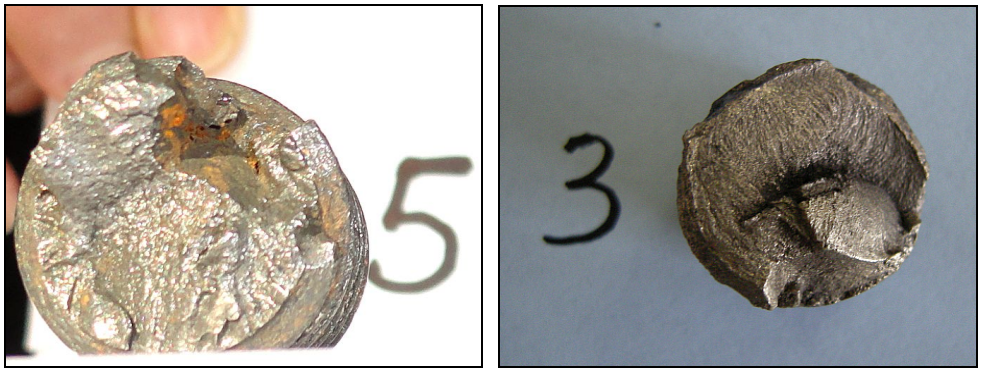

Figure 2. The appearance of fractured surfaces of BB No.5 (Figure 1b) and BB No.3 (Figure 1c). The fractured surfaces are approximately 20 nm gold coated.

3.2. Chemical Analysis

The representative average chemical compositions of materials of RBs and BBs are given in Table 1. The chemical compositions of RB and BB are in limits with requirements of ASTM standard. However, the manganese content of BBs is approximately $\Delta Mn = Mn_{BB} - Mn_{RB} \approx 0.2$ wt.% lower in comparison to RB, and the sulphur content is higher by a factor of three. Although the content of S meets the ASTM requirement, the difference in sulphur content between BB and RB is significant.

Table 1. The average chemical composition of bolt samples [wt.%]

Material Designation	Chemical elements							
	C	Si	Mn	P	S	Cr	Mo	Fe
ASTM A 193 B7	0,37-0,49	0,15-0,35	**0,65-1,10**	< 0,04	**< 0,04**	0,70-1,20	0,15-0,25	balance
RB	0,43	0,26	**0,802**	0,011	**0,005**	1,087	0,208	balance
BB	0,41	0,33	**0,615**	0,013	**0,013**	0,958	0,151	balance

3.3. Mechanical properties

Representative results of mechanical testing are presented in Table 2. Yield strength ($Rp_{0.2}$) and tensile strength (R_m) of RB and BB are in accordance to ASTM standards and meet the criteria for material A 193 B7. Elongation (A) of BB is less than the minimum elongation (A_{min}) set by ASTM standard and it is lower than that for RB. The yield strength and tensile strength of BB are $\Delta R = R_{BB} - R_{RB} \approx 250$ MPa higher, and hardness for $\Delta HV5 = HV5_{BB} - HV5_{RB} \approx 50 - 60$ MPa.

Table 2. Mechanical properties at room temperature

Material Designation	Mechanical properties				
	$R_{p0.2}$ [MPa]	R_m [MPa]	A [%]	Z [%]	HV5 (middle/→/periphery)
ASTM A193 B7	min.720	min.860	min.16	/	…/…/…
RB	833	918	17.5	/	.../291/...
BB	1100	1170	12,5	51	401/341/353

3.4. Primary and secondary structure

The representative apperance of primary structures (Figure 4) shows distributions of suphur- and phosphorus-containing areas which were not atacked by Oberhoffer's reagent (white regions in Figure 4b and Figure 4d). It is obvious a higher S- and P-segregations presence in the case of BB (Figure 4d) in comparison to those of RB (Figure 4b), which are more evently distributed. By comparing the Figure 4a and Figure 4c the segregations are apparently more present in the case of BB (Figure 4c).

Secondary structure of both, RB and BB, consists probably of tempered martensite/bainite structures (dark etched areas), with small ferrite presence (white non-etched areas). There is a possibility that certain amount of pearlite is present, also. Bainite presence is possible if during quenching the cooling rate was lower than critical cooling rate for start of martensite transformation. Pearlite could have been formed from retained austenite during tempering procedure.

Appearance of secondary structure is similar when Figure 4a and Figure 4b are visually compared. Mechanical properties strongly depend on secondary structure. The values of mechanical properties of RB and BB differ significantly (see section 3.3), which suggest that there can be a possibility for some important differences in RB and BB secondary structure properties. More detailed analysis needs to be performed.

3.5. SEM Fractography

Figure 5 gives representative appearance of fractured surfaces of RB and BB tensile specimens. Both fractured surfaces have similar rosette-like appearance. The crack initiation site is at the centre of fibrous area and direction of propagation follows the radial ridges towards periphery. Both fractures have ductile appearance. In Figure 5a it can be observed that central fibrous zone is larger in comparison to that in Figure 5b. The radial ridges are more pronounced, also. These observations suggest that BB tensile specimens are less ductile than those of RB [6]. In addition, although here not presented, the

microfractography results have shown larger presence of cleavage facets on the BB than on RB fractured surface. Fracture mode can be characterized as dimple rupture and micromechanism as microvoid coalescence in the case of RB. The mixed presence of dimples and cleavage facets was noticed in the case of BB tensile specimens.

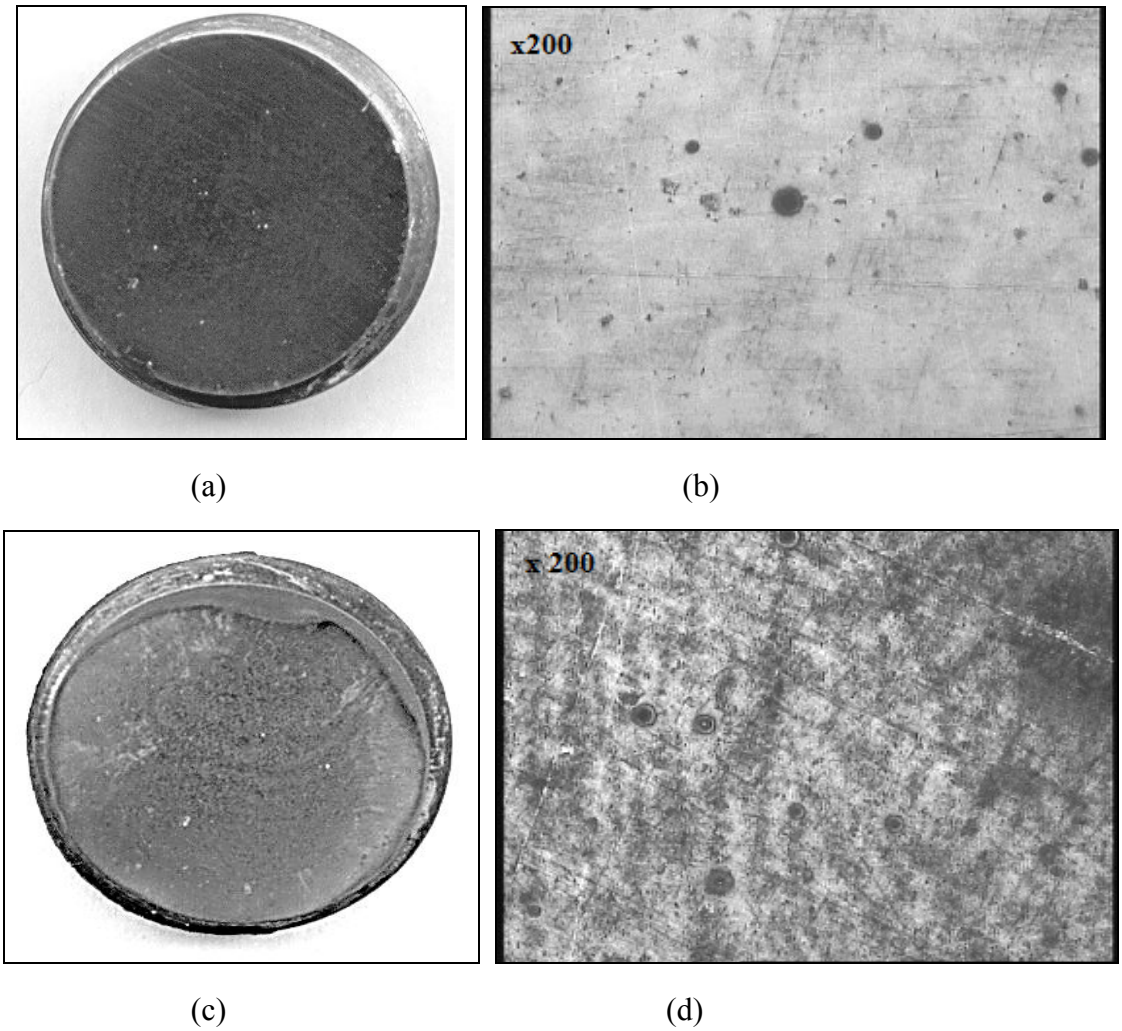

Figure 3. Cross-sectional photomicrographs of primary structure of RB (a) and (b), and BB (c) and (d).

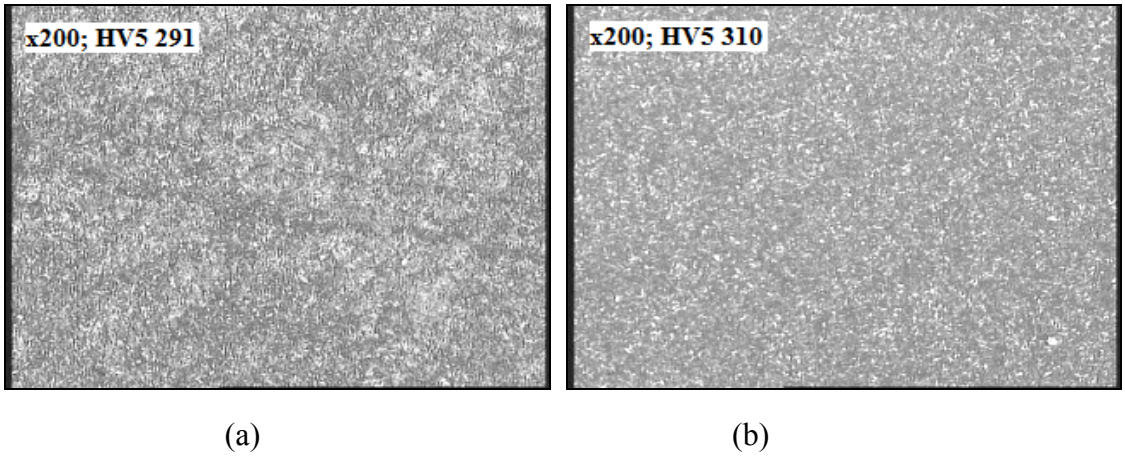

Figure 4. Cross-sectional photomicrographs of secondary structure of RB (a), and BB (b).

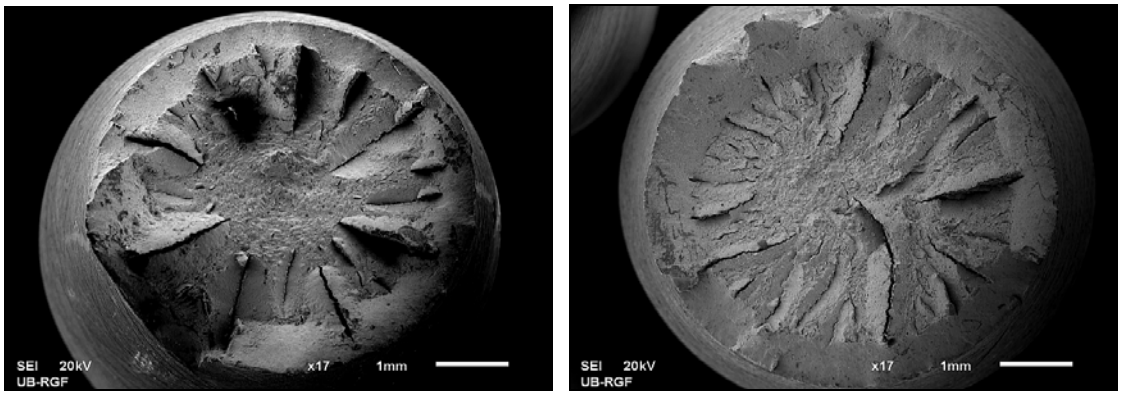

(a) (b)

Figure 5. Macrofractographs of fractured surfaces of RB (a) and BB (b) tensile specimens. Secondary electron images.

In almost all cases, fracture initiation occurred at the root of the screw thread, which is shown by open circles (○) in Figure 6. Also, it can be seen the change in direction of propagation indicated with the open circle at bottom right part of the figure. Straight arrows indicate the direction of crack propagation. Arc curves show the parts of the step-shape surface indicating the possibility that the propagation of fracture took place gradually in several stages. Full circles (●) represent areas of the final fracture. The general appearance of fracture is intergranular brittle-like. The micromechanism of fracture is difficult to determine because the fractured surface is covered with corrosion products (see section 3.6, Figure 8a).

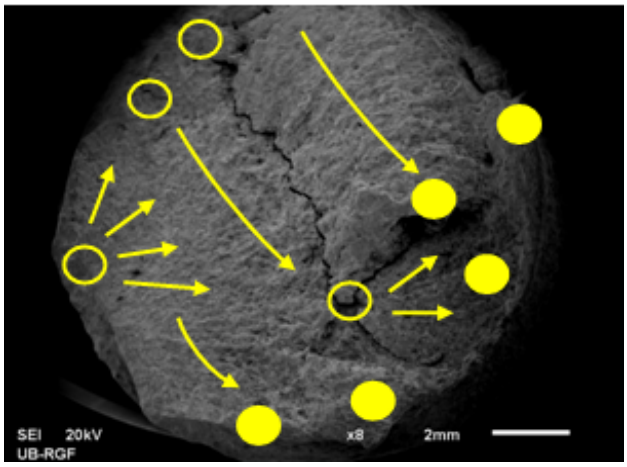

Figure 6. Macrofractograph of fractured surface of BB during exploitation. Secondary electron image.

3.6. SEM-EDS analysis of bolt deposite and fractured surface

In Figure 7 it is shown the qualitative deposite chemistry analysis. The upper right part of Figure 7 is bolt thread side, while lower left side is part of the polished surface on the circumferential side of bolt radial cross-section. Here, the typical morphology of deposite can be observed. Spectrum 1 and 2 (Table 3) show presence of elements typical for bolt material (see also Table 2). Higher amount of carbon is considered as EDS measurement error. Chlorine- and sulphur-containing particles were identified and they are clearly presented in Table 3. Other EDS spectrums show presence of sulphur-containing species.

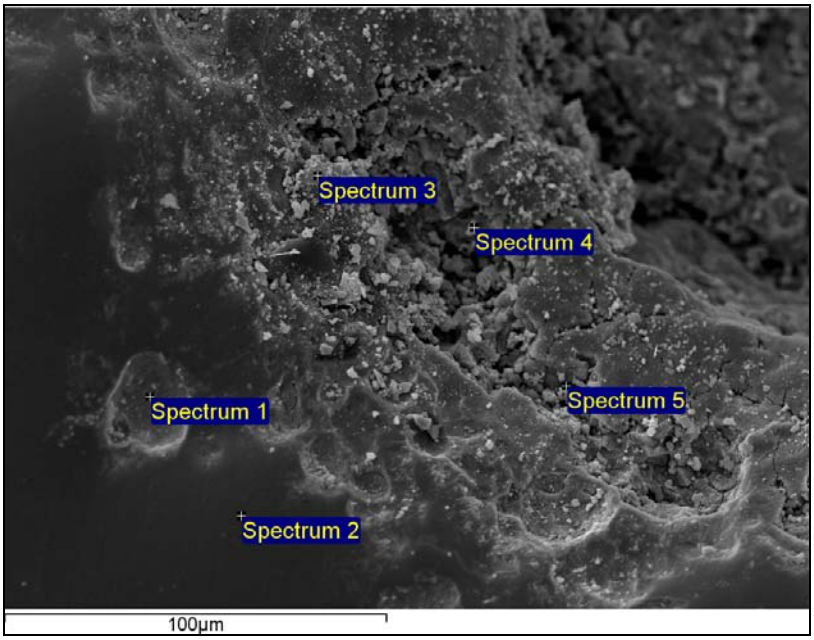

Figure 7. SEM-EDS single-point analysis of bolt deposite chemistry. Secondary electron image.

Table 3. EDS spectrum chemical composition of in wt.% corresponding to Figure 7.

	C	O	Na	Mg	Al	S	Cl	K	Ca	Cr	Mn	Fe	Cu	Total
Spectrum 1	7.37	2.87			0.49					1.30		87.97		100.00
Spectrum 2	17.36									1.04	0.55	81.05		100.00
Spectrum 3		*38.85*	*5.27*		*2.78*	*13.42*	*5.64*	*1.25*	*0.74*			*32.04*		*100.00*
Spectrum 4	*16.80*	*17.27*			*0.64*	*10.26*				*0.91*		*54.12*		*100.00*
Spectrum 5	*14.50*	*36.65*		*0.30*	*0.72*	*3.53*			*0.28*	*1.06*		*42.40*	*0.56*	*100.00*

Figure 8a shows locations of areas where EDS analysis was performed. In Figure 8b the characteristic X-ray Kα peak for sulphur can be observed. This peak is located near Kα for gold. However, by careful analysis it was concluded that belongs to sulphur.

For failure to happen by sulphide stress cracking (SSC) it is necessary presence of 1) aggresive environment i.e. H_2S, 2) susceptible material, 3) sustained tensile stress and 4) electrolite i.e. water or moisture [1].

The results obtained after SEM-EDS analysis of both, bolt deposite and fractured surfaces chemistry revealed that there is an indication of presence of corrosive environment. Beside sulphur-containing species, which indicate on possible presence of H_2S, the chlorine-containing species are identified, also, indicating on possible presence of HCl. Although only a presence of H_2S is sufficient for failure to happen [1,2], the additional presence of HCl could enchance this effect [5].

According to Ref. [1], steels with hardness >22 HRC (equivalent to 550 MPa yield strength) are susceptible to SSC. Obtained results after room-temperature mechanical testing (Table 2) show that both, RB and BB, are susceptible to SSC. The measured yield strength and hardness supersede mentioned levels for SSC susceptibility. The measured yield strength levels of roughly 850-1150 MPa in quenched and tempered state are too high to exclude the fact that these bolts were made of material that was in rolled condition

before quenching and tempering was applied. Yield strength levels for rolled, quenched and tempered state of CrMo steel are reported in Ref. [7,8].

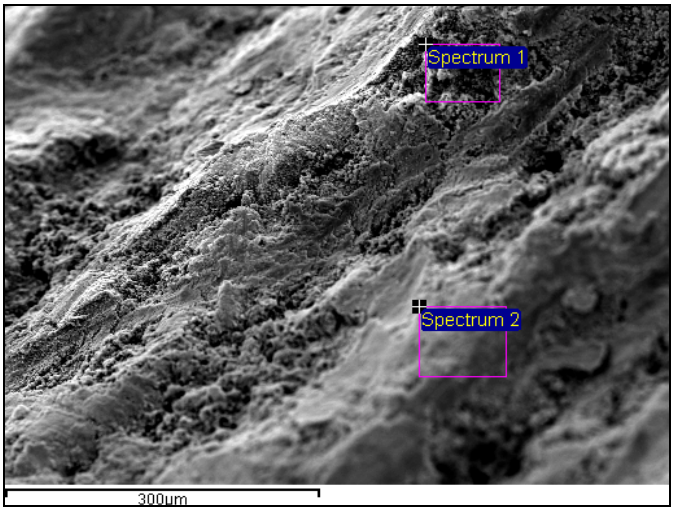

(a)

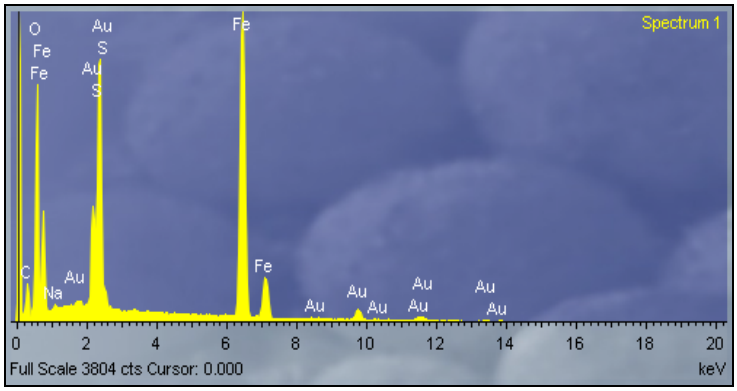

(b)

Figure 8. SEM-EDS area-analysis of fractured surface chemistry. Detail of fractured surface (a) and EDS spectrum (b) corresponding to Figure 8a. Secondary electron image.

When hardness and yield strength values of BB and RB are compared, the 50-60 HV5 and roughly 250 MPa yield strength difference is detected in favour of BB (see section 3.4). This difference is significant and it is way above measurement errors. Also, the elongation is 5% lower. These data indicate on lower ductility of BB in comparison to RB. Also, the results from fractography suggest the same conclusion.

The apparent reason for difference in strength and ductility properties remains unknown. It could be the result of bolt metal processing, cold working (deformation strengthening) or hydrogenation process and subsequent hydrogen embrittlement during exploitation. The later effect is studied recently by Siddiqui et al. [2], where room-temperature mechanical properties were measured as a function of hydrogenation time. It was obtained the increase in strength levels on the order of 100 MPa for 8 h of hydrogenation, and decrease in elongation by approximately 2 %. The exact time which the BB have been exposed to possible corrosion environment is unknown.

The results of primary structure shows the higher level of inhomogeneities present in BB than in RB. Chemical analysis shows the higher sulphur content of BB is detected. In BB was observed appreciable higher presence of microcavities, as well. These results point towards conclusion that quality of BB material is lower than RB and that its fracture resistance is reduced due to existence of unwanted impurity segregations and defects.

4. Conclusions

The preliminary analysis of floating-head heat exchanger bolts failure is carried out. The SEM-EDS analysis of bolts deposite and fractured surface chemistry indicates that corrosion environment was present during the bolts failure. Probably it was environment containing H_2S and HCl. However, in order to confirm such assumptions, detailed analysis on corrosion environment needs to be performed as well as on presence of sources of tensile stresses during the exploitation. The mechanical testing has shown that bolt material was susceptible to possible sulphide stress cracking. Reduced potential for fracture resistance is observed through presence of volume microcavities and primary structure inhomogenity, as well through analyzed fractured surfaces. It was detected higher hardness values of broken bolts in comparison to reference bolts on the order of 50-60 HV5 and higher strength levels of approximately 250 MPa. It was assumed that higher strength levels and lower ductility of broken bolts is the result either of metal processing, cold deformation strengthening or hydrogenation process and hydrogen embrittlement during their exploitation. Apparent reasons are unknown and need to be clarified. It will be done through detailed analysis of structure properties, effects of cold working conditions and hydrogenation process on room-temperature mechanical properties.

Acknowledgments

This work was co-financed from the Ministry of Education and Science of Republic of Serbia (project No. TR 34028).

References

1. F. Nasirpouri, H. Alizadeh, M. Hosseingholizadeh, *Failure analysis of a carbon steel screw under the service in the presence of hydrogen sulphide,* Engineering Failure Analysis, xxx (2011) xxx-xxx, Article in Press.
2. R.A. Siddiqui, Hussein A. Abdullah, *Hydrogen embrittlement in 0.31% carbon steel used for petrochemical applications,* Journal of Materials Processing Technology 170 (2005) 430-435.
3. N. Nanninga, J. Grochowsi, L. Heldt, K. Rundman, *Role of microstructure, composition and hardness in resisting hydrogen embrittlement of fastener grade steels,* Corrosion Science 52 (2010) 1237-1246.
4. Jarmila Woodtli, Rolf Kieselbach, *Damage due to hydrogen embrittlement and stress corrosion cracking,* Energy Failure Analysis 7 (2000) 427-450.
5. Junwen Tang, Yawei Shao, Tao Zhang, Guozhe Meng, Fuhui Wanga, *Corrosion behaviour of carbon steel in different concentrations of HCl solutions containing H_2S at 90°C,* Corrosion Science 53 (2011) 1715-1723.
6. N. Saeidi, A. Ekrami, *Comparison of mechanical properties of martensite/ferrite and bainite/ferrite dual phase 4340 steels*, Materials Science and Engineering A 523 (2009) 125-129.
7. M.Gojić, L. Kosec, P. Matković, *The effects of tempering temperature on mechanical properties and microstructure of low alloy Cr and CrMo steel*, Journal of Material Science 33 (1998) 395-403.
8. Woei Shyuan Lee, Tzai-Tian Su, *Mechanical properties and microstructural features of AISI 4340 high-strength alloy steel under quenched and tempered condition*, Journal of Materials Processing Technology 87 (1999) 198-206.